Quantum Critical Dynamics of a Heisenberg-Ising Chain in a Longitudinal Field: Many-Body Strings versus Fractional Excitations

Zhe Wang,[1,*] M. Schmidt,[2] A. Loidl,[2] Jianda Wu,[3,†] Haiyuan Zou,[3] Wang Yang,[4] Chao Dong,[5,6] Y. Kohama,[5] K. Kindo,[5] D. I. Gorbunov,[7] S. Niesen,[8] O. Breunig,[8] J. Engelmayer,[8] and T. Lorenz[8]

[1]*Institute of Radiation Physics, Helmholtz-Zentrum Dresden-Rossendorf, 01328 Dresden, Germany*
[2]*Experimental Physics V, Center for Electronic Correlations and Magnetism, Institute of Physics, University of Augsburg, 86135 Augsburg, Germany*
[3]*Tsung-Dao Lee Institute and School of Physics and Astronomy, Shanghai Jiao Tong University, Shanghai 200240, China*
[4]*Stewart Blusson Quantum Matter Institute, University of British Columbia, Vancouver, Canada*
[5]*Institute for Solid State Physics, University of Tokyo, Kashiwa, Chiba 277-8581, Japan*
[6]*Wuhan National High Magnetic Field Center and School of Physics, Huazhong University of Science and Technology, Wuhan 430074, China*
[7]*Dresden High Magnetic Field Laboratory (HLD-EMFL), Helmholtz-Zentrum Dresden-Rossendorf, 01328 Dresden, Germany*
[8]*Institute of Physics II, University of Cologne, 50937 Cologne, Germany*

(Received 13 March 2019; published 6 August 2019)

We report a high-resolution terahertz spectroscopic study of quantum spin dynamics in the antiferromagnetic Heisenberg-Ising spin-chain compound $BaCo_2V_2O_8$ as a function of temperature and longitudinal magnetic field. Confined spinon excitations are observed in an antiferromagnetic phase below $T_N \simeq 5.5$ K. In a field-induced gapless phase above $B_c = 3.8$ T, we identify many-body string excitations as well as low-energy fractional psinon or antipsinon excitations by comparing to Bethe ansatz calculations. In the vicinity of B_c, the high-energy string excitations are found to have a dominant contribution to the spin dynamics as compared with the fractional excitations.

DOI: 10.1103/PhysRevLett.123.067202

Understanding quantum critical dynamics in strongly correlated many-body systems is a compelling and challenging task in modern condensed-matter physics [1–6]. For example, the onset of unconventional superconductivity is proximate to a quantum critical point, which is featured by enhanced spin fluctuations due to the suppression of long-range antiferromagnetic order by external parameters, e.g., hole doping in copper oxides [2] or applied pressure in heavy fermion systems [4]. In frustrated and/or low-dimensional quantum magnets, even without the complication of charge correlations, exotic spin states, such as quantum spin liquids [5] or a magnonic Bose-Einstein condensate [6], emerge at quantum phase transitions [1]. However, the corresponding critical dynamics is generally elusive, and, in particular, the role of high-energy excitations, such as many-body bound states of magnons [7–10], remains to be clarified, as compared to the well-established low-energy fractionalized spin excitations [11,12].

A paradigmatic spin-interaction model to investigate the quantum critical dynamics is the one-dimensional (1D) spin-1/2 Heisenberg-Ising (or XXZ) model

$$J\sum_{i}^{N}[(S_i^xS_{i+1}^x+S_i^yS_{i+1}^y)+\Delta S_i^zS_{i+1}^z]-g\mu_BB\sum_{i}^{N}S_i^z, \quad (1)$$

with nearest-neighbor antiferromagnetic exchange interaction $J > 0$. In a longitudinal magnetic field, this integrable model allows for a precise calculation of the many-body spin dynamics [7–10,13–19] as well as of the ground state [20]. In the large-Ising-anisotropy ($\Delta > 1$) or high-field ($B > B_s$) limit (see Fig. 1), the spin dynamics is characterized by gapped excitations on top of an antiferromagnetic or a field-polarized ferromagnetic ground state, respectively. While the latter has particlelike magnon (or spin wave) excitations of integer quantum number $S = 1$, the former is featured by a continuum of spinon-pair excitations with fractionalized quantum number $S = 1/2$. As tuning into the gapless regime from different directions, one can naturally expect richer spin dynamics due to strongly enhanced spin fluctuations, especially for small magnetizations.

Indeed, it has been theoretically shown that, in the XY limit $|\Delta| < 1$, not only two-spinon but also four-spinon excitations contribute significantly to the spin dynamics [15]. For the isotropic Heisenberg model ($\Delta = 1$), even high-energy Bethe (or Bethe-Gaudin-Takahashi) string states (complex magnon bound states [7–10]) possess a certain weight in the transverse sector of the dynamic structure factor [17]. Although the multiple fractional excitations were observed by inelastic neutron scattering experiments in various Heisenberg spin-chain compounds [21–24], an observation of the high-energy string excitations remains challenging to a scattering experiment. Alternatively, by using local quantum quenches, signatures of

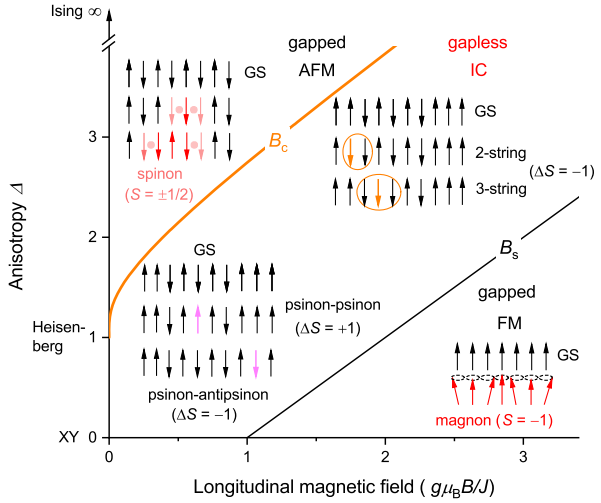

FIG. 1. Phase diagram of the antiferromagnetic XXZ spin-1/2 chain with the anisotropy parameter Δ in a longitudinal magnetic field. The different regimes (gapped or gapless) are separated by the critical field B_c and saturation field B_s and are characterized by distinct ground states (GS) and characteristic excitations due to a spin flip, as schematically illustrated by the insets.

string states can appear in time-dependent nonequilibrium dynamics [25,26] and were indeed evidenced in a cold-atom experiment for $\Delta \approx 1$ [27]. However, it is far from obvious how to realize the quench dynamics in a condensed-matter experiment.

In the relatively underexplored Ising-like regime ($\Delta > 1$), in contrast, a recent theoretical work [19] found that even in equilibrium the high-energy string states can have a considerable contribution to the spin dynamics in the field-induced gapless phase ($B_c < B < B_s$). In particular, close to the critical line $B = B_c$, where quantum spin fluctuations are extremely strong, the string states should be detectable by a scattering experiment. Our experimental approach here is to carry out high-resolution terahertz (THz) spectroscopic measurements on the Ising-like spin-1/2 chain compound $BaCo_2V_2O_8$ in an applied longitudinal magnetic field. By tracking sharp resonance absorption lines as a function of the magnetic field and comparing it to a Bethe ansatz calculation, we unambiguously determine many-body strings and fractional spin excitations. This further allows us to identify the dominant excitations governing the quantum critical dynamics.

The realization of strong spin anisotropy has been found in many Co^{2+}-based materials [28–41]. In $BaCo_2V_2O_8$, the spin chains with a fourfold screw axis running along the crystallographic c axis are formed by edge-shared CoO_6 octahedra. Because of spin-orbit coupling and crystal-field effects, interactions between the effective $S = 1/2$ Co^{2+} ions in $BaCo_2V_2O_8$ can be described by the 1D antiferromagnetic XXZ model with an Ising-like anisotropy also along the c axis [41–47]. High-quality single crystals prepared by the floating-zone method [43] were studied by longitudinal-field ($B\|c$) magnetization and magnetocaloric-effect measurements, in pulsed fields with a rise time of 7 and 14 ms, respectively, and a pulse duration of 20 and 36 ms. Quasiadiabatic conditions were maintained for the magnetocaloric-effect measurements [48].

As shown in Fig. 2(a), starting from 1.7 K at zero field, the sample temperature $T(B)$ reaches a minimum at $B_c = 3.8$ T, which is followed by a slight increase towards higher fields. Before the temperature increases drastically above $B_s = 22.9$ T, there is a weak minimum around $B_h = 19.5$ T, which corresponds to the half-saturated magnetization [see Fig. 2(b)] and reflects commensurate fluctuations [45]. With down-sweeping the field, $T(B)$ follows very well the up-sweeping curve, apart from a heating effect in the 3D ordered phase. At elevated temperatures, the minima at B_h and B_c rapidly broaden and disappear, whereas the minimum at B_s remains sharp and

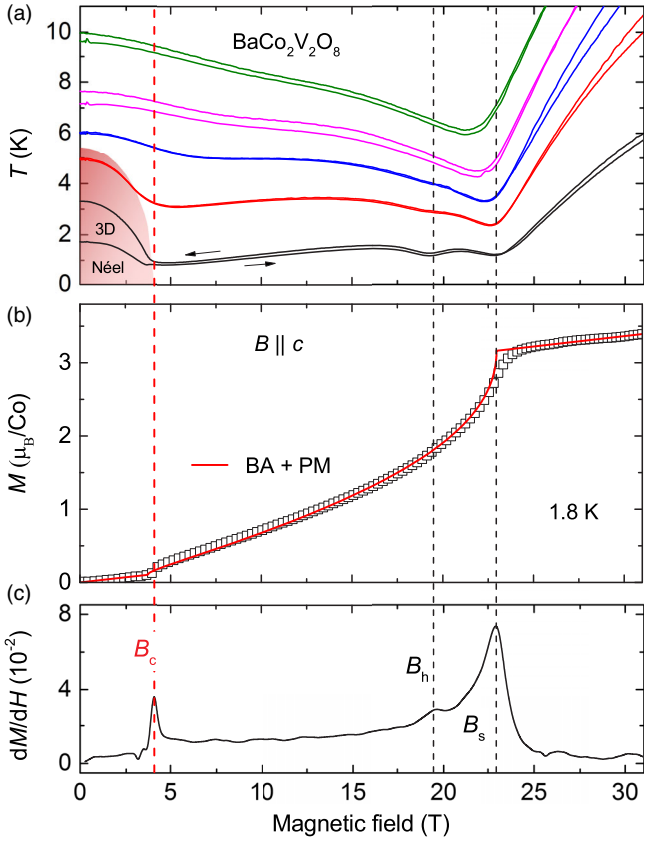

FIG. 2. (a) Magnetocaloric-effect $T(B)$, (b) magnetization $M(B)$, and (c) differential susceptibility dM/dH measured as a function of longitudinal field $B\|c$. The critical field $B_c = 3.8$ T and the characteristic fields $B_h = 19.5$ and $B_s = 22.9$ T corresponding to half-saturated and saturated magnetizations, respectively, yield minima of $T(B)$ and peaks of dM/dH at the lowest temperature, as marked by the dashed lines. In (a), the shaded area indicates the 3D Néel ordered phase [43]. In (b), the solid line is obtained from a Bethe ansatz (BA) solution of the Heisenberg-Ising model, in addition to a paramagnetic (PM) background.

becomes the only dominant feature above T_N. These features qualitatively agree with the phase diagram expected for the 1D Heisenberg-Ising model (Fig. 1). This is also reflected by the magnetization results, which are quantitatively reproduced by the 1D Heisenberg-Ising model with $J = 2.6$ meV, $\Delta = 2.17$, and $g = 6.2$, in addition to a weak paramagnetic background with $\chi_{pm} = 0.028\mu_B/T$ [solid line, Fig. 2(b)]. As will be seen below, this parameter set simultaneously provides an excellent description of the observed spin dynamics.

Dynamical properties were obtained by measuring THz transmission spectra on single crystals with a typical size of $4 \times 4 \times 0.5$ mm^3, using a commercial time-resolved spectrometer (Toptica Photonics/TeraFlash). Dependence on the longitudinal field ($B\|c$) was acquired up to 7 T in Faraday geometry with a magneto-optical cryostat (Oxford Instruments/Spectromag).

Transmission spectra above and below T_N are shown in Fig. 3(a) for $h^\omega \perp c$, $e^\omega \| c$. The spectra are dominated by a strong phonon band between 5 and 7 meV, and at 2 K (below T_N) additional absorption peaks are observed at 1.6 and 2.5 meV as indicated by the arrows. In contrast, in the available spectral range, the spectra for the cross polarization $h^\omega \| c$ and $e^\omega \perp c$ are essentially featureless [49]. Therefore, the observed phonon is active only for $e^\omega \| c$, while the low-energy excitations are magnetic and active for $h^\omega \perp c$. The observed selection rule for the magnetic excitations reflects the Ising anisotropy of the antiferromagnetic order [45,46].

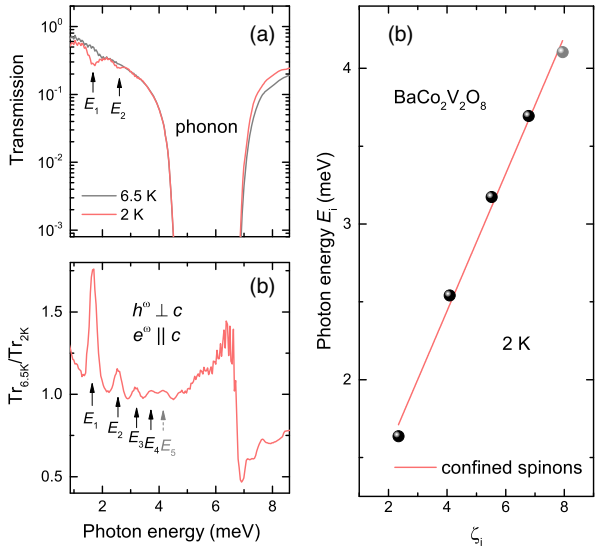

FIG. 3. (a) Transmission spectra measured at 6.5 and 2 K, above and below $T_N \simeq 5.5$ K, respectively, for the polarization $h^\omega \perp c$, $e^\omega \| c$. (b) The ratio of the transmission spectra at 6.5 and 2 K reveals absorption peaks, as indicated by the arrows, which signal the excitations of confined spinons below T_N. (c) The energy hierarchy of these excitations linearly depends on ζ_i, as expected for confined spinons in a linear confining potential [34].

Besides a broad peak feature at 5–7 meV [Fig. 3(b)], corresponding to a slight temperature-dependent shift of the phonon band, the ratio of the 6.5 and 2 K transmission spectra exhibits a series of peaks (E_i, $i = 1, 2, 3, 4, 5$) at lower energies, appearing below the magnetic phase transition at $T_N \simeq 5.5$ K. While the E_5 mode is weak and tentatively assigned, the $E_1, \ldots, E_4$ modes are confirmed also in the field-dependent experiment [see Fig. 4(b)]. As expected for the excitations of confined spinons [31–36,42], the energy hierarchy of these modes clearly follows the linear dependence on ζ_i, $E_i = 2E_0 + \zeta_i \lambda^{2/3}(\hbar^2/\mu)^{1/3}$, $i = 1, 2, 3, \ldots$, where ζ_i are the negative zeros of the Airy function $\mathrm{Ai}(-\zeta_j) = 0$, μ is the effective mass, λ measures the confining potential, and $2E_0$ is the threshold energy for creating two spinons [50]. The linear fit in Fig. 3(d) gives $2E_0 = 0.68(10)$ meV and $\lambda^{2/3}(\hbar^2/\mu)^{1/3} = 0.44(2)$ meV. While the latter is comparable to the value determined at finite momentum transfers by inelastic neutron scattering [51], the threshold energy is lower here, because the lower boundary of the spinon-pair continuum has a minimum at the Γ point. Moreover, instead of an overwhelming excitation continuum above $2E_1$, the observation of the high-lying confined spinons, i.e., $E_4 > 2E_1$ [and their field dependence; see Fig. 4(b)], is a distinct fingerprint of confinement effects in an Ising-like spin chain [52].

In the longitudinal field, we observe a Zeeman splitting of the confined spinon states, which all follow a similar field dependence towards B_c with a g factor of 5.7(1). The softening of the lowest-lying confined-spinon level signals the field-induced quantum phase transition to a gapless phase, as expected for the 1D XXZ model (see Fig. 1). Since these features have been discussed in previous works [34,38,42], we will focus on the spin dynamics above and close to the quantum phase transition at $B_c = 3.8$ T.

In the gapless regime above B_c, excitations with different field dependencies are revealed, signaling very different dynamical properties. As indicated by the arrows in Fig. 4(a), four modes corresponding to transmission minima can be followed at different fields [49]. With an increasing field, while the mode $R^{pp}_{\pi/2}$ softens, the frequencies of the modes R^{pap}_0, $\chi^{(2)}_\pi$, and $\chi^{(3)}_{\pi/2}$ increase. To compare these experimental results to theory, we performed Bethe ansatz calculations of the transverse dynamic structure factors (DSFs) $S^{a\bar{a}}(q,\omega) = \pi \sum_\mu |\langle \mu | S^{\bar{a}}_q | G \rangle|^2 \delta(\omega - E_\mu + E_G)$ [19], where $S^\pm_q = (1/\sqrt{N}) \sum_N e^{iqn} S^\pm_n$ and $\bar{a} = -a$ with $a = +$ or $-$. $S^\pm_n \equiv S^x_n \pm S^y_n$ is a spin operator acting on the spin site n. The ground state and excited state are expressed by $|G\rangle$ and $|\mu\rangle$ with eigenenergies of E_G and E_μ, respectively. Since the transmission measurements were performed in Faraday geometry, i.e., $h^\omega \perp B$, the calculated transverse DSFs right correspond to the spin-flip excitations induced by linear coupling to the THz magnetic field h^ω.

Usually, THz spectroscopy probes only the vicinity of the Γ point (zero-momentum transfer). As the spin chain in

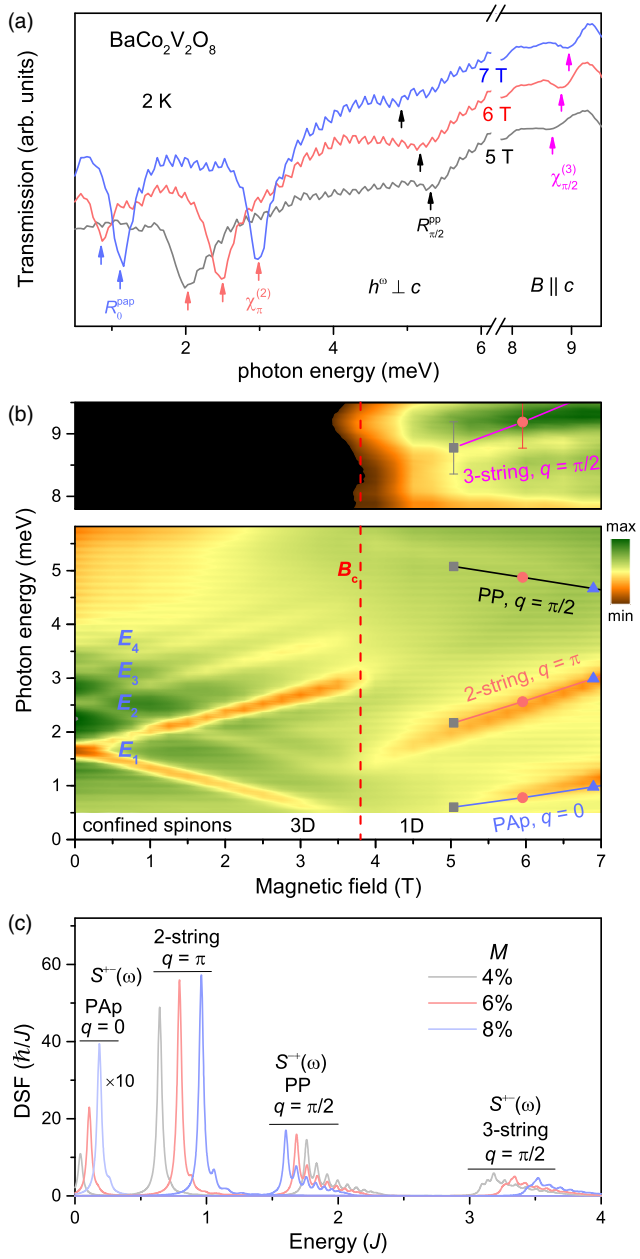

FIG. 4. (a) Transmission spectra obtained at 2 K in the longitudinal fields above B_c. Excitations of 2-string $\chi_\pi^{(2)}$, 3-string $\chi_{\pi/2}^{(3)}$, psinon-antipsinon R_0^{pap} pairs, and psinon-psinon $R_{\pi/2}^{pp}$ pairs are indicated, as identified by comparing to Bethe ansatz results. The weak wigglelike feature is due to multiple interference within the sample. (b) Contour plot of transmission at 2 K. For $B < B_c$, confined-spinon levels E_i are observed. For $B > B_c$, different excitations with distinct slopes are observed, as for the string and fractional excitations. The symbols above B_c show fitting of the theory results in (c) (see the text for details). A different color scale is adopted in the upper panel to highlight the weak 3-string mode. (c) Dynamic structure factors (DSF) S^{+-} and S^{-+} as a function of the energy, obtained via Bethe ansatz for the magnetizations 4%, 6%, and 8% of the saturated value. The units are given by the Planck constant $\hbar$ and the exchange interaction J. For clarity, the DSF for pap is multiplied by a factor of 10.

$BaCo_2V_2O_8$ has a four-step screw symmetry along the chain direction [41], we evaluated not only for $q = 0$ but also for $q = \pi$ and $\pi/2$ in order to account for the zone-folding effects. The dominant modes obtained with a narrow line shape are shown in Fig. 4(c). According to the Bethe ansatz solution, these are excitations of psinon-antipsinon (pap) pairs, psinon-psinon (pp) pairs, length-2 strings, and length-3 strings. As illustrated schematically in the inset in Fig. 1 ($B_c < B < B_s$), while the psinons or antipsinons are domain-wall-like fractional excitations, the 2-string and 3-string excitations are complex magnon bound states of two and three magnons, respectively [7–10,19]. By performing Bethe ansatz calculations at different magnetizations (or equivalent magnetic fields) [49], we derive characteristic field dependencies of the various sharp excitations [see Fig. 4(c)], which allows us to unambiguously identify the experimentally observed excitations.

As shown in Fig. 4(b), the Bethe ansatz results can be very well compared to the observed excitations above B_c, with the same set of parameter as for fitting the magnetization [Fig. 2(b)]. The resonance frequencies of these modes follow very nicely the theoretically expected linear dependence on the magnetic field above 5 T. To take into account the nonlinear dependence approaching B_c, the theory results are shifted upward by a constant of 0.5 meV, which is smaller than the lower-energy limit of our spectroscopy. The overall excellent comparison allows us to identify the experimentally observed modes as fractional psinon or antipsinon excitations as well as 2-string and 3-string excitations, as marked in Figs. 4(a) and 4(b). The revealed selection rule is summarized in Table I.

Comparing the intensities with the fractional excitations, the 2-string mode turns out to have unique features. From Fig. 4(a), it is, first of all, obvious that the pap and 2-string modes are much sharper and stronger than the pp and 3-string modes. Second, with a decreasing field, the intensity of the low-energy pap modes significantly decreases, while the field dependence of the 2-string mode is less pronounced. Third, approaching B_c from above, the 2-string mode becomes finally dominant over the low-energy pap mode. While the first two features have also been observed by a previous study in a related compound $SrCo_2V_2O_8$ [37],

TABLE I. Selection rule for the observed confined spinons, psinon-psinon (pp), psinon-antipsinon (pap), and string excitations.

$H\|\|c$	ΔS	$h^\omega \perp c$	$h^\omega \|\| c$
Confined spinons	± 1	Yes	No
pp	$+1$	Yes	
pap	-1	Yes	
2-string	-1	Yes	
3-string	-1	Yes	

the third observation, which is the most important experimental finding of the present work, cannot be made by using the electron spin resonance (ESR) spectroscopy of Ref. [37]. In an ESR spectrum, the resonance for the different modes occurs always at different fields, which hinders a direct comparison among the different modes.

Conventionally, the theory of Tomonaga-Luttinger liquid has been well established to properly describe quantum fluctuations in the critical regime for a large variety of systems [53], such as the spin-1/2 XXZ chain with easy-plane anisotropy and the spin-1/2 strong-leg spin ladder [54]. In contrast, our experimental observations, being consistent with the Bethe ansatz results [see Fig. 4(c)] [19], show that the string excitations have a dominant contribution to the critical dynamics as approaching B_c in the paradigmatic mode of the 1D spin-1/2 antiferromagnetic Heisenberg-Ising model. Therefore, a comprehensive description of the quantum critical dynamics requires going beyond the theory of Tomonaga-Luttinger liquid.

In conclusion, we have identified exotic spin excitations, such as many-body string and fractional excitations, and revealed their selection rule in the vicinity of a field-induced quantum phase transition in the Ising-like spin-1/2 chain compound $BaCo_2V_2O_8$. Below the phase transition, the spin dynamics is characterized by gapped fractional spinon excitations with strong confinement features. In contrast, above the phase transition in the gapless phase, the dominant role is played by the high-energy string excitations, although low-energy fractional excitations of psinons or antipsinons are present as well. Our results provide a guide for hunting high-energy string excitations, e.g., by photon or neutron scattering, and suggest that the high-energy many-body excitations may generally play an important role in quantum critical dynamics.

We thank Congjun Wu for fruitful discussions. We acknowledge partial support by the DFG (German Research Foundation) via project No. 107745057 Transregio 80: From Electronic Correlations to Functionality (Subproject F5) and via Project No. 277146847—Collaborative Research Center 1238: Control and Dynamics of Quantum Materials (Subprojects No. A02 and No. B01). The high field experiments at Dresden were supported by HLD at HZDR, member of the European Magnetic Field Laboratory (EMFL). Z. W. acknowledges hospitality of ISSP, the University of Tokyo, and of Tsung-Dao Lee Institute. J. W. acknowledges additional support from a Shanghai talent program.

*zhewang@ph2.uni-koeln.de
Present address: Institute of Physics II, University of Cologne, 50937, Cologne, Germany.
†wujd@sjtu.edu.cn

[1] S. Sachdev, Quantum magnetism and criticality, Nat. Phys. **4**, 173 (2008).
[2] B. Keimer, S. A. Kivelson, M. R. Norman, S. Uchida, and J. Zaanen, From quantum matter to high-temperature superconductivity in copper oxides, Nature (London) **518**, 179 (2015).
[3] H. v. Löhneysen, A. Rosch, M. Vojta, and P. Wölfle, Fermi-liquid instabilities at magnetic quantum phase transitions, Rev. Mod. Phys. **79**, 1015 (2007).
[4] P. Gegenwart, Q. Si, and F. Steglich, Quantum criticality in heavy-fermion metals, Nat. Phys. **4**, 186 (2008).
[5] L. Balents, Spin liquids in frustrated magnets, Nature (London) **464**, 199 (2010).
[6] T. Giamarchi, Ch. Rüegg, and O. Tchernyshyov, Bose-Einstein condensation in magnetic insulators, Nat. Phys. **4**, 198 (2008).
[7] H. Bethe, Zur Theorie der metalle. I. Eigenwerte und eigenfunktionen der linearen atomkette, Z. Phys. **71**, 205 (1931).
[8] M. Gaudin, Thermodynamics of the Heisenberg-Ising Ring for $\Delta \geq 1$, Phys. Rev. Lett. **26**, 1301 (1971).
[9] M. Takahashi and M. Suzuki, One-dimensional anisotropic Heisenberg model at finite temperatures, Prog. Theor. Phys. **48**, 2187 (1972).
[10] M. Takahashi, *Thermodynamics of One-Dimensional Solvable Models* (Cambridge University Press, Cambridge, England, 2005).
[11] L. D. Faddeev and L. A. Takhtajan, What is the spin of a spin wave?, Phys. Lett. A **85**, 375 (1981).
[12] H. Shiba, Quantization of magnetic excitation continuum due to interchain coupling in nearly one-dimensional Ising-like antiferromagnets, Prog. Theor. Phys. **64**, 466 (1980).
[13] N. Kitanine, J. M. Mailet, and V. Terras, Form factors of the XXZ Heisenberg spin-1/2 finite chain, Nucl. Phys. **B554**, 647 (1999).
[14] M. Karbach and G. Müller, Line-shape predictions via Bethe ansatz for the one-dimensional spin-1/2 Heisenberg antiferromagnet in a magnetic field, Phys. Rev. B **62**, 14871 (2000).
[15] J.-S. Caux, R. Hagemans, and J. M. Maillet, Computation of dynamical correlation functions of Heisenberg chains: The gapless anisotropic regime, J. Stat. Mech. (2005) P09003.
[16] R. G. Pereira, S. R. White, and I. Affleck, Exact Edge Singularities and Dynamical Correlations in Spin-1/2 Chains, Phys. Rev. Lett. **100**, 027206 (2008).
[17] M. Kohno, Dynamically Dominant Excitations of String Solutions in the Spin-1/2 Antiferromagnetic Heisenberg Chain in a Magnetic Field, Phys. Rev. Lett. **102**, 037203 (2009).
[18] M. T. Batchelor, The Bethe ansatz after 75 years, Phys. Today **60**, No. 1, 36 (2007).
[19] W. Yang, J. Wu, S. Xu, Z. Wang, and C. Wu, Quantum spin dynamics of the axial antiferromagnetic spin-1/2 XXZ chain in a longitudinal magnetic field, arXiv:1702.01854v1.
[20] C. N. Yang and C. P. Yang, One-dimensional chain of anisotropic spin-spin interactions. II. Properties of the ground-state energy per lattice site for an infinite system, Phys. Rev. **150**, 327 (1966).
[21] B. Lake, D. A. Tennant, J.-S. Caux, T. Barthel, U. Schollwöck, S. E. Nagler, and C. D. Frost, Multispinon Continua at Zero and Finite Temperature in a Near-Ideal Heisenberg Chain, Phys. Rev. Lett. **111**, 137205 (2013).

[22] M. Mourigal, M. Enderle, A. Klöpperpieper, J.-S. Caux, A. Stunault, and H. M. Rønnow, Fractional spinon excitations in the quantum Heisenberg antiferromagnetic chain, Nat. Phys. **9**, 435 (2013).

[23] B. Lake, D. A. Tennant, C. D. Frost, and S. E. Nagler, Quantum criticality and universal scaling of a quantum antiferromagnet, Nat. Mater. **4**, 329 (2005).

[24] M. B. Stone, D. H. Reich, C. Broholm, K. Lefmann, C. Rischel, C. P. Landee, and M. M. Turnbull, Extended Quantum Critical Phase in a Magnetized Spin-1/2 Antiferromagnetic Chain, Phys. Rev. Lett. **91**, 037205 (2003).

[25] M. Ganahl, E. Rabel, F. H. L. Essler, and H. G. Evertz, Observation of Complex Bound States in the Spin-1/2 Heisenberg XXZ Chain Using Local Quantum Quenches, Phys. Rev. Lett. **108**, 077206 (2012).

[26] W. Liu and N. Andrei, Quench Dynamics of the Anisotropic Heisenberg Model, Phys. Rev. Lett. **112**, 257204 (2014).

[27] T. Fukuhara, P. Schauß, M. Endres, S. Hild, M. Cheneau, I. Bloch, and Ch. Gross, Microscopic observation of magnon bound states and their dynamics, Nature (London) **502**, 76 (2013).

[28] M. E. Lines, Magnetic Properties of $CoCl_2$ and $NiCl_2$, Phys. Rev. **131**, 546 (1963).

[29] V. J. Folen, J. J. Krebs, and M. Rubenstein, Magnetic properties of K_2CoF_4, a highly anisotropic two-dimensional magnetic structure, Solid State Commun. **6**, 865 (1968).

[30] H. Shiba, Y. Ueda, K. Okunishi, S. Kimura, and K. Kindo, Exchange interaction via crystal-field excited states and its importance in $CsCoCl_3$, J. Phys. Soc. Jpn. **72**, 2326 (2003).

[31] R. Coldea, D. A. Tennant, E. M. Wheeler, E. Wawrzynska, D. Prabhakaran, M. Telling, K. Habicht, P. Smeibidl, and K. Kiefer, Quantum Criticality in an Ising chain: Experimental evidence for emergent E8 symmetry, Science **327**, 177 (2010).

[32] C. M. Morris, R. Valdés Aguilar, A. Ghosh, S. M. Koohpayeh, J. Krizan, R. J. Cava, O. Tchernyshyov, T. M. McQueen, and N. P. Armitage, Hierarchy of Bound States in the One-Dimensional Ferromagnetic Ising Chain $CoNb_2O_6$ Investigated by High-Resolution Time-Domain Terahertz Spectroscopy, Phys. Rev. Lett. **112**, 137403 (2014).

[33] M. Mena, N. Hänni, S. Ward, E. Hirtenlechner, R. Bewley, C. Hubig, U. Schollwöck, B. Normand, K. W. Krämer, D. F. McMorrow, and Ch. Rüegg, Thermal control of spin excitations in the coupled Ising-chain material $RbCoCl_3$, arXiv:1811.07178.

[34] Z. Wang, M. Schmidt, A. K. Bera, A. T. M. N. Islam, B. Lake, A. Loidl, and J. Deisenhofer, Spinon confinement in the one-dimensional Ising-like antiferromagnet $SrCo_2V_2O_8$, Phys. Rev. B **91**, 140404(R) (2015).

[35] Z. Wang, J. Wu, S. Xu, W. Yang, C. Wu, A. K. Bera, A. T. M. N. Islam, B. Lake, D. Kamenskyi, P. Gogoi, H. Engelkamp, N.-L. Wang, J. Deisenhofer, and A. Loidl, From confined spinons to emergent fermions: Observation of elementary magnetic excitations in a transverse-field Ising chain, Phys. Rev. B **94**, 125130 (2016).

[36] A. Bera, B. Lake, F. H. L. Essler, L. Vanderstraeten, C. Hubig, U. Schollwöck, A. T. M. N. Islam, A. Schneidewind, and D. L. Quintero-Castro, Spinon confinement in a quasi-one dimensional anisotropic Heisenberg magnet, Phys. Rev. B **96**, 054423 (2017).

[37] Z. Wang, J. Wu, W. Yang, A. K. Bera, D. Kamenskyi, A. T. M. N. Islam, S. Xu, J. M. Law, B. Lake, C. Wu, and A. Loidl, Experimental observation of Bethe strings, Nature (London) **554**, 219 (2018).

[38] Q. Faure, S. Takayoshi, S. Petit, V. Simonet, S. Raymond, L.-P. Regnault, M. Boehm, J. S. White, M. Månsson, Ch. Rüegg, P. Lejay, B. Canals, T. Lorenz, S. C. Furuya, T. Giamarchi, and B. Grenier, Topological quantum phase transition in the Ising-like antiferromagnetic spin chain, Nat. Phys. **14**, 867 (2018).

[39] O. Breunig, M. Garst, E. Sela, B. Buldmann, P. Becker, L. Bohaty, R. Müller, and T. Lorenz, The Spin-1/2 XXZ Chain System Cs_2CoCl_4 in a Transverse Magnetic Field, Phys. Rev. Lett. **111**, 187202 (2013).

[40] O. Breunig, M. Garst, A. Rosch, E. Sela, B. Buldmann, P. Becker, L. Bohaty, R. Müller, and T. Lorenz, Low-temperature ordered phases of the Spin-1/2 XXZ chain system Cs_2CoCl_4, Phys. Rev. B **91**, 024423 (2015).

[41] Z. He, D. Fu, T. Kyômen, T. Taniyama, and M. Itoh, Crystal growth and magnetic properties of $BaCo_2V_2O_8$, Chem. Mater. **17**, 2924 (2005).

[42] S. Kimura, H. Yashiro, K. Okunishi, M. Hagiwara, Z. He, K. Kindo, T. Taniyama, and M. Itoh, Field-Induced Order-Disorder Transition in Antiferromagnetic $BaCo_2V_2O_8$ Driven by a Softening of Spinon Excitation, Phys. Rev. Lett. **99**, 087602 (2007).

[43] S. K. Niesen, G. Kolland, M. Seher, O. Breunig, M. Valldor, M. Braden, B. Grenier, and T. Lorenz, Magnetic phase diagrams, domain switching, and quantum phase transition of the quasi-one-dimensional Ising-like antiferromagnet $BaCo_2V_2O_8$, Phys. Rev. B **87**, 224413 (2013).

[44] S. K. Niesen, O. Breunig, S. Salm, M. Seher, M. Valldor, and T. Lorenz, Substitution effects on the temperature vs. magnetic-field phase diagrams of the quasi-1D effective Ising spin-1/2 chain system $BaCo_2V_2O_8$, Phys. Rev. B **90**, 104419 (2014).

[45] M. Klanjšek, M. Horvatić, S. Krämer, S. Mukhopadhyay, H. Mayaffre, C. Berthier, E. Canévet, B. Grenier, P. Lejay, and E. Orignac, Giant magnetic field dependence of the coupling between spin chains in $BaCo_2V_2O_8$, Phys. Rev. B **92**, 060408(R) (2015).

[46] B. Grenier, V. Simonet, B. Canals, P. Lejay, M. Klanjšek, M. Horvatić, and C. Berthier, Neutron diffraction investigation of the H–T phase diagram above the longitudinal incommensurate phase of $BaCo_2V_2O_8$, Phys. Rev. B **92**, 134416 (2015).

[47] Z. Wang, T. Lorenz, D. I. Gorbunov, P. T. Cong, Y. Kohama, S. Niesen, O. Breunig, J. Engelmayer, A Herman, Jianda Wu, K. Kindo, J. Wosnitza, S. Zherlitsyn, and A. Loidl, Quantum Criticality of an Ising-like Spin-1/2 Antiferromagnetic Chain in a Transverse Magnetic Field, Phys. Rev. Lett. **120**, 207205 (2018).

[48] T. Kihara, Y. Kohama, Y. Hashimoto, S. Katsumoto, and M. Tokunaga, Adiabatic measurements of magneto-caloric effects in pulsed high magnetic fields up to 55 T, Rev. Sci. Instrum. **84**, 074901 (2013).

[49] See Supplemental Material at http://link.aps.org/supplemental/10.1103/PhysRevLett.123.067202 for transmission spectra and for magnetization from Bethe ansatz calculations.

[50] B. M. McCoy and T. T. Wu, Two-dimensional Ising field theory in a magnetic field: Breakup of the cut in the two-point function, Phys. Rev. D **18**, 1259 (1978).

[51] B. Grenier, S. Petit, V. Simonet, E. Canévet, L.-P. Regnault, S. Raymond, B. Canals, C. Berthier, and P. Lejay, Longitudinal and Transverse Zeeman Ladders in the Ising-Like Chain Antiferromagnet $BaCo_2V_2O_8$, Phys. Rev. Lett. **114**, 017201 (2015).

[52] A. J. A. James, R. M. Konik, and N. J. Robinson, Nonthermal States Arising from Confinement in One and Two Dimensions, Phys. Rev. Lett. **122**, 130603 (2019).

[53] F. D. M. Haldane, General Relation of Correlation Exponents and Spectral Properties of One-Dimensional Fermi Systems: Application to the Anisotropic $S = 1/2$ Heisenberg Chain, Phys. Rev. Lett. **45**, 1358 (1980).

[54] T. Giamarchi, Some experimental tests of Tomonaga-Luttinger liquies, Int. J. Mod. Phys. B **26**, 1244004 (2012).